processes

MDPI

Article

Economic and Exergy Assessments for Ocean Thermal Energy Conversion Using Environment-Friendly Fluids

Hongbo Lu [1], Chengcheng Fan [2], Deming Li [2], Yongping Chen [2] and Feng Yao [3,*]

[1] School of Management, Beijing Institute of Technology, Beijing 100081, China
[2] School of Energy and Environment, Southeast University, Nanjing 210096, China
[3] Key Laboratory of Efficient Low-Carbon Energy Conversion and Utilization of Jiangsu Provincial Higher Education Institutions, School of Environmental Science and Engineering, Suzhou University of Science and Technology, Suzhou 215009, China
* Correspondence: yaofeng@usts.edu.cn

Abstract

It is of particular interest to use eco-friendly working fluids in ocean thermal energy conversion (OTEC) systems. In response, this study develops a thermo-economic model to evaluate the feasibility of fourth-generation refrigerants, including R1234yf, R1234ze(Z), and R1336mzz(Z), as potential alternatives to ammonia. The analysis examines the effects of system scale and cold seawater pumping depth on capital investment distribution and key economic indicators, such as the levelized cost of energy (*LCOE*) and net present value (*NPV*). The findings highlight the viability of R1234ze(Z) as a substitute for ammonia, demonstrating a slightly lower *LCOE* and requiring 8.6% less installed capacity to achieve financial breakeven. Additionally, the economic impact of pumping depth varies with system scale: in small-scale OTEC systems, *LCOE* initially decreases with depth before rising beyond an optimal point, while in large-scale systems, it continuously declines and eventually stabilizes. Moreover, capital investment allocation shifts with system size, making pipeline optimization crucial for small-scale systems, whereas minimizing heat exchanger costs is key to enhancing the economic feasibility of large-scale OTEC plants. The results offer guidance for cost-effective OTEC deployment and refrigerant selection, supporting a sustainable energy supply for tropical islands.

Keywords: ocean thermal energy conversion; economic performance; net present value; levelized cost of energy

Academic Editor: Christos Argirusis

Received: 30 July 2025
Revised: 20 August 2025
Accepted: 25 August 2025
Published: 29 August 2025

Citation: Lu, H.; Fan, C.; Li, D.; Chen, Y.; Yao, F. Economic and Exergy Assessments for Ocean Thermal Energy Conversion Using Environment-Friendly Fluids. *Processes* **2025**, *13*, 2780. https://doi.org/10.3390/pr13092780

1. Introduction

In tropical and subtropical areas, ocean thermal energy is abundantly available as a temperature difference between the warm surface seawater and the cold water in deeper layers. It possesses abundant reserves, with an estimated global power potential of up to 10 TW. Moreover, under the backdrop of rising global temperatures, the power potential for ocean thermal energy is projected to increase by an additional 46% by the end of this century [1]. In addition, compared to most intermittent renewable energy sources such as wind and solar power, ocean thermal energy is less affected by environmental fluctuations, enabling a nearly continuous and stable energy output. Consequently, harnessing ocean thermal energy presents significant potential for contributing to carbon neutrality objectives [2,3].

The concept of harnessing ocean thermal energy via conversion systems was originally proposed by French scientist D'Arsonval in 1881. Fifty years later, Georges Claude built

a 22 kW land-based ocean thermal energy conversion (OTEC) power plant, marking the world's first OTEC platform. In 1935, Georges Claude attempted to construct a floating OTEC power platform using a barge near the coast of Brazil, but the project was abandoned due to adverse weather conditions. Following this setback, research on OTEC remained largely stagnant for several decades. Over the past 50 years, however, OTEC technology has regained attention, particularly from maritime nations such as the United States and Japan [4–7]. Notably, a 100 kW OTEC facility was successfully put into operation by Japan on Kumejima Island in 2013 [8], while the United States established a 100 kW OTEC facility in Hawaii in 2014 [9], both of which have achieved continuous operation and represent the state of the art in OTEC development. More recently, in 2023, China successfully developed a 20 kW floating OTEC power generation system and completed its sea trials in the South China Sea. Currently, OTEC systems predominantly use ammonia as the working fluid due to its favorable thermodynamic properties. However, ammonia also presents several critical drawbacks, including high toxicity and flammability, which pose significant safety and environmental risks, particularly for large-scale and offshore applications [10,11]. Therefore, identifying alternative working fluids that combine environmental friendliness with superior thermodynamic characteristics is essential for advancing OTEC development.

The small temperature difference in OTEC results in relatively low thermal efficiency and poor economic performance. Therefore, the primary criteria for selecting a working fluid are its thermodynamic and economic performance [12–14]. Sun et al. [15] established a thermodynamic model of an OTEC system utilizing the organic Rankine cycle (ORC), and demonstrated that ammonia outperforms R134a as a working fluid by delivering greater net power output. Subsequently, Yoon et al. [16] conducted a broader comparative analysis of 12 potential working fluids, including R134a, ammonia, R22, R290, R600a, R1270, R744, R245fa, R227ea, R236fa, R410A, and R404A. Their results showed that ammonia-based systems achieved the highest thermal efficiency, reaching 2.72%. While acknowledging ammonia's high efficiency, they also highlighted its toxicity, which poses potential environmental risks. To address these concerns, Vera et al. [17] expanded the selection criteria for OTEC working fluids by considering not only conventional refrigerants but also more environment-friendly fourth-generation fluids, such as R1234yf, R1234ze, propane, and isobutene. Similarly, Huo et al. [18] examined working fluid selection for a hybrid solar-OTEC trigeneration system, incorporating fourth-generation refrigerants R1234ze(E) and R1234yf. However, these studies did not investigate the economic performance of OTEC systems, which is a critical factor given the inherently low thermal efficiency of OTEC. In general, ammonia continues to be the favored option for ensuring both thermodynamic efficiency and economic viability in OTEC systems. However, considering long-term operation and environmental sustainability, selecting high-performance working fluids from third- and fourth-generation refrigerants presents a viable alternative.

In summary, ocean thermal energy, as a renewable energy source with abundant reserves and stable output, plays a crucial role in building a zero-carbon energy system and achieving carbon neutrality. However, while ammonia, the most commonly used working fluid in OTEC systems, offers superior thermodynamic properties, its high toxicity and strong corrosiveness present significant challenges for the large-scale construction of offshore platforms. Therefore, a comparative study on the performance differences between environment-friendly working fluids and ammonia in OTEC systems, along with a comprehensive thermodynamic and economic assessment of OTEC systems using environment-friendly working fluids, is essential for developing a clean, efficient, and economically viable OTEC system. To address this, this study establishes a thermo-economic model for OTEC systems and compares the economic performance of OTEC systems utilizing R1234yf, R1234ze(Z), R1336mzz(Z), and ammonia. Additionally, the

feasibility of R1234ze(Z) as a potential alternative to ammonia is analyzed, with considerations including economies of scale, the impact of seawater intake depth, and capital investment distribution.

2. System Description

Ocean thermal energy conversion (OTEC) systems generate electricity by exploiting the temperature difference between warm surface seawater and cold deep seawater. The effectiveness of OTEC systems depends on the temperature difference between surface and deep seawater, typically requiring a gradient of at least 20 °C. This renewable energy technology is especially beneficial in tropical and subtropical regions, where consistent temperature differences are present.

Figure 1 is a schematic diagram of ocean thermal energy conversion. The system operates through a closed thermodynamic cycle consisting of key components, including a warm water heat exchanger (evaporator), a turbine, a generator, a cold water heat exchanger (condenser), and a working fluid pump. Warm surface seawater transfers heat to the working fluid in the evaporator, causing the fluid to vaporize. The high-pressure vapor powers a turbine linked to a generator, transforming thermal energy into mechanical energy, which is then converted into electricity. After passing through the turbine, the vapor enters the condenser, where it is cooled and condensed into a liquid by the heat exchange with cold deep seawater. The liquid working fluid is subsequently returned to the evaporator, thus completing the cycle.

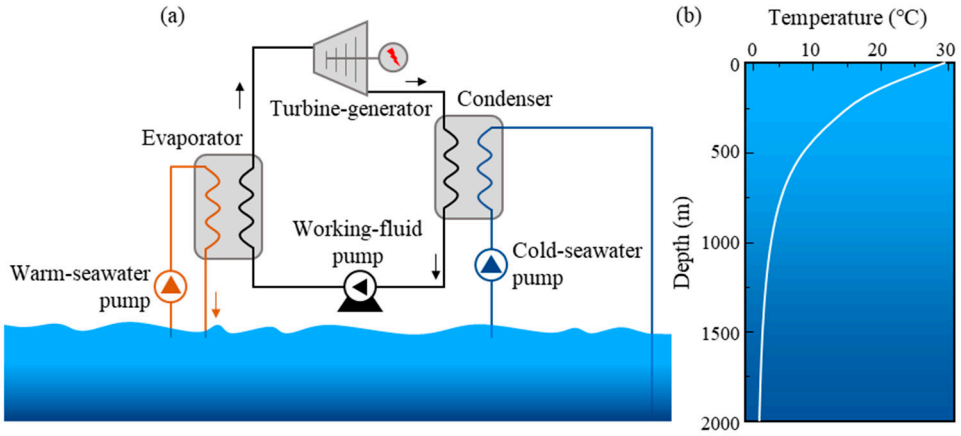

Figure 1. Schematic diagram of ocean thermal energy conversion and ocean thermocline: (**a**) working principal; (**b**) ocean thermocline [19].

Ammonia (R717) has been widely used as the working fluid in OTEC systems due to its low boiling point, high latent heat of vaporization, and favorable thermodynamic properties, which enable efficient operation in low-temperature difference conditions. However, despite these advantages, ammonia exhibits several critical drawbacks, including high toxicity and flammability, posing significant risks to operational safety and environmental protection, especially in large-scale and offshore applications. Consequently, there is a growing interest in exploring fourth-generation refrigerants, such as HFO-1234yf, HFO-1234ze(Z), and HFO-1336mzz(Z), as potential replacements for ammonia.

Fourth-generation refrigerants, primarily hydrofluoroolefins (HFOs), offer several advantages over ammonia. Firstly, these fluids are environmentally friendly, featuring ultra-low global warming potentials (GWPs) and zero ozone depletion potentials (ODPs). Secondly, HFOs exhibit improved safety profiles, with low toxicity and reduced flammability compared to ammonia, enhancing operational safety in OTEC systems deployed near residential or ecologically sensitive areas. Moreover, these fluids possess favorable

thermodynamic properties that can match or even surpass ammonia in low-temperature applications, enabling high thermal efficiencies and reduced pumping power requirements. In summary, while ammonia remains the standard working fluid in OTEC systems, its inherent limitations necessitate the exploration of alternative refrigerants. Fourth-generation refrigerants such as HFO-1234yf, HFO-1234ze(Z), and HFO-1336mzz(Z) represent a significant advancement in addressing environmental, safety, and performance challenges. Further research and development are essential to optimize their integration into OTEC systems and unlock their full potential for sustainable energy generation. The thermodynamic properties of the HFOs considered in this paper are listed in Table 1.

Table 1. Thermodynamic properties of selected fluids.

Fluids	Critical Pressure (MPa)	Critical Temperature (°C)	ODP (kgCFC-11eq)	GWP ($kgCO_2$-eq)
R717	11.33	132.3	0	/
HFO-1234yf	3.38	94.7	0	<1
HFO-1234ze(Z)	3.52	165.5	0	<1
HFO-1336mzz(Z)	2.90	171.3	0	2

3. Methodology

3.1. Thermo-Economic Model Development

Thermo-economic modeling integrates thermodynamic and economic analyses to evaluate the feasibility and cost-effectiveness of OTEC systems. This section details the development of a comprehensive model for assessing OTEC systems, including the formulation of thermodynamic equations and a cost estimation method. The basic assumptions are as follows:

(1) The system is assumed to operate continuously under steady-state conditions;
(2) Pressure losses in heat exchangers and pipelines are neglected;
(3) Heat transfer between heat exchangers/pipelines and the surrounding environment is neglected;
(4) Exergy calculations are referenced to a state of 101 kPa and 20 °C.

3.1.1. Thermodynamic Model

The OTEC system considered in this study is a closed-cycle configuration, comprising key components such as an evaporator, turbine, condenser, and pumps. In this system, the working fluid undergoes a continuous cycle involving heat exchange between warm/cold seawater and working fluid, energy conversion in the turbine, and fluid transportation through the working fluid pump.

(1) Evaporator

The working fluid captures heat from the warm seawater and transitions from liquid to vapor within the evaporator. In accordance with the law of energy conservation,

$$\begin{cases} Q_{\text{eva}} = c_{\text{P}} \dot{m}_{\text{ww}} (T_{\text{ww,in}} - T_{\text{ww,out}}) \\ Q_{\text{eva}} = \dot{m}_{\text{wf}} (h_{\text{wf,out}} - h_{\text{wf,in}}) \\ Q_{\text{eva}} = U_{\text{eva}} A_{\text{eva}} \Delta T \end{cases} \quad (1)$$

where Q_{eva} is heat transfer through the evaporator, c_{P} is specific heat capacity of seawater, $\dot{m}_{\text{ww}}$ and $\dot{m}_{\text{wf}}$ are flow rate of warm seawater and working fluid, $T_{\text{ww,in}}$ and $T_{\text{ww,out}}$ are temperatures of warm seawater at evaporator the inlet and outlet, respectively, and $h_{\text{wf,in}}$ and $h_{\text{wf,out}}$ are the specific enthalpies of working fluid at the evaporator inlet and outlet, respectively. A_{eva} is heat transfer area of the evaporator, ΔT is heat transfer tem-

perature difference between the working fluid and warm seawater, and U is overall heat transfer coefficient.

(2) Condenser

In the condenser, the working fluid is condensed by releasing heat to the cold seawater. According to the law of energy conservation,

$$\begin{cases} Q_{con} = c_P \dot{m}_{cw}(T_{cw,out} - T_{cw,in}) \\ Q_{con} = \dot{m}_{cw}(h_{wf,in} - h_{wf,out}) \\ Q_{con} = U_{con} A_{con} \Delta T \end{cases} \quad (2)$$

where Q_{con} is heat transfer through the condenser, $\dot{m}_{cw}$ and $\dot{m}_{wf}$ are flow rate of cold seawater and working fluid, $T_{cw,in}$ and $T_{cw,out}$ are temperatures of cold seawater at the condenser inlet and outlet, respectively, and $h_{wf,in}$ and $h_{wf,out}$ are the specific enthalpies of the working fluid at the condenser inlet and outlet, respectively. A_{con} is heat transfer area of the evaporator, ΔT is heat transfer temperature difference between the working fluid and warm seawater, and U_{con} is overall heat transfer coefficient.

(3) Turbine-generator

The turbine's power output is directly dependent on the effective enthalpy drop of the working fluid and can be expressed as

$$P_{tur} = \dot{m}_{wf}(h_{tur,in} - h_{tur,out}) = \dot{m}_{wf}\eta_{tur,is}(h_{tur,in} - h_{tur,out,is}) \quad (3)$$

where, subscript "tur" denotes the turbine, while "in" and "out" represent the inlet and outlet, respectively, and $\eta_{tur,is}$ is the isentropic efficiency of the turbine, a key parameter that characterizes turbine performance. In thermodynamic cycle driven by small temperature differences, this efficiency typically averages around 70% and varies with operating conditions. For simplification, this study assumes a constant isentropic efficiency of 70%, which is a common assumption in OTEC studies.

(4) Working Fluid Pump

The working fluid pump is responsible for transporting the working fluid between the condenser and the evaporator. Its power consumption is directly determined by the mass flow rate of the working fluid and the pressure difference across the pump and can be expressed as

$$P_{WFP} = \dot{m}_{wf}(h_{wf,out} - h_{wf,in}) = \dot{m}_{wf}(h_{wf,out,is} - h_{wf,in})\eta_{WFP} \quad (4)$$

where η_{WFP} is isentropic efficiency of the working fluid pump.

(5) Seawater Pump

The power consumption of the warm seawater pump and the cold seawater pump is determined by the pressure losses associated with the flow of warm and cold seawater, respectively. Therefore, the power consumption of the seawater pump, $W_{WWP/CWP}$, can be expressed as

$$P_{WWP/CWP} = \frac{m_{ww/cw}\left(\Delta P_{eva/con} + \Delta P_{WWpipe/CWpipe}\right)}{\rho_{sw}\eta_{WP}} \quad (5)$$

where subscript "WWP" and "CWP" denote warm seawater pump and cold seawater pump, subscript "eva" and "con" denote evaporator and condenser, subscript "WWpipe" and "CWpipe" are warm seawater pipe and cold seawater pipe. ΔP is the pressure drop, ρ_{sw} is density of seawater, and η_{WP} is the efficiency of seawater pump.

The friction loss of seawater inside the heat exchanger is primarily due to local resistance at the entry and exit and frictional resistance during flow inside.

The friction loss in the heat exchanger mainly results from local resistance at the entry and exit points, ΔP_M, and frictional resistance during flow, ΔP_F.

$$\Delta P_{eva/con} = \Delta P_M + \Delta P_F \quad (6)$$

$$\Delta P_M = 1.5\frac{V^2}{2v} \quad (7)$$

$$\Delta P_F = 4f_{HX}\frac{L\rho}{D_h}\frac{V^2}{2} \quad (8)$$

where V and v are the fluid velocity and specific volume, respectively, L is the plate length, and f_{HX} is the friction factor and can be obtained by [20,21]

$$f_{HX} = 2.99/\mathrm{Re}^{0.385} \quad (9)$$

The friction loss of seawater inside the pipeline can be calculated by

$$\Delta P_{pipe} = f_P\frac{l}{d}\frac{v^2}{2g} \quad (10)$$

where l and d are length and diameter of seawater pipe, g is gravitational acceleration, and f_p can be determined as follows [19]:

$$f = \frac{0.25}{\log^2\left(\frac{z}{3.7d} + \frac{5.74}{\mathrm{Re}^{0.9}}\right)} \quad (11)$$

The thermodynamic parameters required for model calculations are listed in Table 2. In the calculations, the pressure loss due to fluid flow in the pipeline and heat exchanger is neglected [19,22], which is a common assumption in OTEC studies, and the efficiencies of the pump and turbine are assumed to be constant, unaffected by changes in operating conditions. Additionally, the heat exchange temperature difference in the evaporator and condenser is set at 2 °C, which is a commonly adopted assumption to ensure the feasibility of the OTEC systems that operate with a small temperature difference. In OTEC systems, the extraction of deep cold seawater poses significant technical challenges due to the complexity of deep-sea operations. Efficient use of cold seawater is crucial for improving the overall energy conversion efficiency and economic viability of OTEC systems. Therefore, in the model formulation, a 4 °C temperature rise in the cold seawater within the condenser ensures effective energy extraction while maintaining a feasible temperature difference for OTEC applications.

The relationship between seawater velocity, heat transfer, and flow resistance in pipelines and heat exchangers is highly complex. However, this study primarily focuses on system investment costs and economic performance rather than detailed flow characteristics. Hence, simplified empirical relationships are used to describe the interactions between seawater velocity, heat transfer coefficient, and flow resistance while neglecting the geometric features such as the inlet/outlet shapes and flow channels of heat exchangers. Specifically, a seawater velocity of 2 m/s in the pipeline is assumed to keep the flow resistance in polyethylene pipes below 100 Pa/m, meeting engineering practice requirements. The seawater velocity in the heat exchanger is assumed to be 1 m/s, and the corresponding flow resistance is determined using the velocity–pressure drop correlation for plate heat exchangers provided in Ref. [23], which is further used to estimate the power consumption of the seawater pump.

Table 2. Specific parameters for thermodynamic model of OTEC system.

Thermodynamic Parameters (Unit)	Values
Warm seawater temperature (°C)	26~31
Pumping depth of cold seawater (m)	400~1800
Pinch point temperature difference (°C)	2
Overall heat transfer coefficient of evaporator ($W/m^2/K$)	1500
Overall heat transfer coefficient of condenser ($W/m^2/K$)	1600
Isentropic efficiency of turbine (%)	80
Isentropic efficiency of pump (%)	70
Seawater pipe length (m)	=Pumping depth of cold seawater
Seawater pipe thickness (m)	0.09
Seawater pipe density (kg/m^3)	995
Seawater pipe roughness (mm)	0.0053
Seawater velocity in pipe (m/s)	1
Seawater velocity in heat exchanger (m/s)	2
Cold seawater temperature rise in condenser (°C)	4

(6) Exergy Balance

In addition to energy, exergy is another key thermodynamic parameter, representing the quality of energy. All the components in the system follow the exergy balance equation, which is expressed as

$$\sum E_{\text{in}} + P_{\text{in}} = \sum E_{\text{out}} + P_{\text{out}} + I \tag{12}$$

where P_{in} is the power consumption, P_{out} is the power output, E_{in} and E_{out} are respectively the input exergy and output exergy, and I is the exergy destruction. Since no chemical reactions are involved in OTEC systems, the E is calculated as:

$$E = \dot{m}[(h - h_0) - T_0(s - s_0)] \tag{13}$$

where h_0, T_0, and s_0 represent the specific enthalpy, temperature, and specific entropy at the reference state, respectively.

3.1.2. Cost Model

The OTEC system considered in this study adopts the most mature configuration, namely the organic Rankine cycle. Therefore, excluding auxiliary components such as valves and working fluid pipelines, the system's initial investment mainly covers the evaporator, condenser, turbine, pumps for the working fluid, warm seawater, and cold seawater, as well as the seawater pipelines. For components other than seawater pipelines, their initial investment costs can be determined based on their key design parameters and the correlation given in Equation (14):

$$C = \frac{CEPCI_{2024}}{CEPCI_{2008}} k_1 (Z/k_2)^{k_3} \tag{14}$$

where C represents the initial investment cost of the component, while Z is the key design parameters. For the evaporator and condenser, Z corresponds to the heat exchange area, whereas for the turbine and pumps, it refers to the power consumption. The constants k_1, k_2, and k_3 vary depending on the component type, with specific values provided in Table 3, noting that the parameters used in this study were originally based on 2008 data. To account for the change in equipment and construction costs over time, the Chemical Engineering Plant Cost Index (CEPCI) has been applied to update the values to 2024 levels.

Specifically, the 2008 CEPCI of 575.4 was adjusted to the 2024 CEPCI of 798.8, following the standard cost-indexing method.

Table 3. Specific parameters for model of ocean thermal energy conversion.

Economic Parameters (Unit)		Values	
Operational and maintenance factor (%)		6	
Annual operating time (h)		8000	
Discount rate (%)		10	
Project lifespan (years)		30	
Electricity price (USD/kWh)		0.12	
Depreciation rate (%)		4	
Tax rate (%)		25	
Cost Estimation Factor	k_1	k_2	k_3
Evaporator	130	0.093	0.78
Condenser	588	1.0	0.8
Turbine	6000	1.0	0.78
Pumps	3540	1.0	0.7

Noting that, the turbine investment cost was modeled as a function of the installed capacity only, without further breakdown into subcomponent-level cost factors. This simplification is consistent with common practice in thermodynamic and techno-economic analyses of OTEC and other renewable energy systems, where the primary objective is to capture the dominant cost–capacity relationship while maintaining model tractability. Given that the focus of this work is on assessing the relative impact of different working fluids on the overall economic performance under identical design and operating conditions, a more detailed subcomponent cost modeling would increase complexity without significantly affecting the comparative conclusions.

For simplicity, the cost estimation of seawater pipelines considers only the material cost, while transportation and installation costs are neglected. The selected material is high-density polyethylene (HDPE), with a fixed pipe wall thickness of 0.09 m [24]. Additionally, although the maximum manufacturable diameter of HDPE pipes is currently 4 m [23], this constraint is not imposed in the actual calculations. Instead, it is assumed that the system consists of a single seawater pipeline. It should be noted that in large-scale OTEC systems, the increase in capacity inevitably requires larger-diameter and thicker-walled HDPE pipes for cold seawater intake, which can introduce manufacturing and deployment challenges, such as extrusion and joining limitations, deformation risks under deep-water hydrostatic pressure, transportation constraints, and higher offshore installation complexity. While these factors may contribute to a disproportionate increase in capital cost and construction time during scale-up, the primary focus of this study is to compare the techno-economic performance of different working fluids under identical design conditions. Therefore, a rigorous treatment of these engineering challenges is beyond the scope of the present work, and they are only briefly discussed here to provide additional context.

3.2. Evaluation Indicators

The thermodynamic performance of ocean thermal energy conversion using environment-friendly fluids is evaluated using exergy efficiency, which is defined as the ratio of net power output to the total exergy input to the system:

$$\eta_{ex} = \frac{P_{tur} - P_{WFP} - P_{WWP} - P_{CWP}}{(E_{ww,in} - E_{ww,out}) + (E_{cw,in} - E_{cw,out})} \quad (15)$$

The economic performance of ocean thermal energy conversion using environment-friendly fluids is assessed using levelized cost of energy (*LCOE*) and net present value (*NPV*). Levelized cost of energy (*LCOE*) is the average cost of generating each unit of electricity throughout an energy project's lifespan. It accounts for capital expenditure, operational and maintenance costs, and discount rates:

$$LCOE = \frac{CRF \times CAPEX + \varphi \times CAPEX}{\tau_0 P_{\text{net}}/1000} \tag{16}$$

where *CAPEX* is the total initial capital investment, φ is the factor corresponding to the operational and maintenance costs, τ_0 is the annual operating time in hours, and P_{net} is net power output.

Capital recovery factor (*CRF*) is a financial coefficient to convert the initial capital investment into an equivalent annual cost over the project's lifetime. It accounts for the time value of money by incorporating the discount rate and project lifespan:

$$CRF = \frac{r(1+r)^n}{(1+r)^n - 1} \tag{17}$$

where r and n are discount rate and project lifespan, respectively.

Net present value (*NPV*) is the difference between the discounted present values of cash inflows and outflows over a specified period, accounting for the time value of money:

$$NPV = -CAPEX + \sum_{t=1}^{n} \frac{(epP_{\text{net}} - \varphi CAPEX - dCAPEX)(1 - tax) + dCAPEX}{(1+r)^t} \tag{18}$$

where *ep* is electricity price, *d* is depreciation rate, and tax is tax rate. The parameter values involved in Equations (2)–(4) are listed in Table 2.

4. Results and Discussion

To comprehensively evaluate the applicability of low-GWP working fluids in OTEC systems, this study first conducts an exergy analysis to assess the thermodynamic performance of four refrigerants: R1234yf, R1234zd(Z), R1336mzz(Z), and the conventional R717. The analysis includes the calculation of component-wise exergy destruction and the overall exergy efficiency of each system configuration. Following the exergy assessment, a detailed techno-economic analysis is performed. The economic performance of each working fluid is examined using levelized cost of energy and net present value as key indicators. The effects of system scale, warm seawater temperature, and cold seawater intake depth on economic metrics are also investigated to identify trade-offs between environmental impact and cost-effectiveness.

4.1. Exergy Analysis

Figure 2 presents the exergy efficiencies of OTEC systems using R717, R1234yf, R1234ze(Z), and R1336mzz(Z) as working fluids under varying surface seawater temperatures. Across all working fluids, the exergy efficiency increases steadily as the surface temperature rises. This behavior is attributed to the enhanced temperature gradient between surface and deep seawater, which strengthens the thermodynamic driving force of the cycle and improves the system's exergy utilization. Among the four refrigerants, R717 consistently shows the highest exergy efficiency throughout the temperature range considered. The other three environment-friendly refrigerants follow in the order of R1336mzz(Z), R1234ze(Z), and R1234yf, with relatively small differences in efficiency between them. For instance, at a surface seawater temperature of 30 °C, the exergy efficiencies are 32.814% for

R717, 32.179% for R1336mzz(Z), 31.458% for R1234ze(Z), and 30.831% for R1234yf. These variations remain within a narrow band across the tested temperature range. The increase in exergy efficiency with surface temperature is observed consistently for all fluids, indicating the positive role of higher surface temperatures in improving the thermodynamic performance of OTEC systems, and the ranking reflects differences in latent heat and vapor density, with R717 offering the most favorable thermodynamic properties.

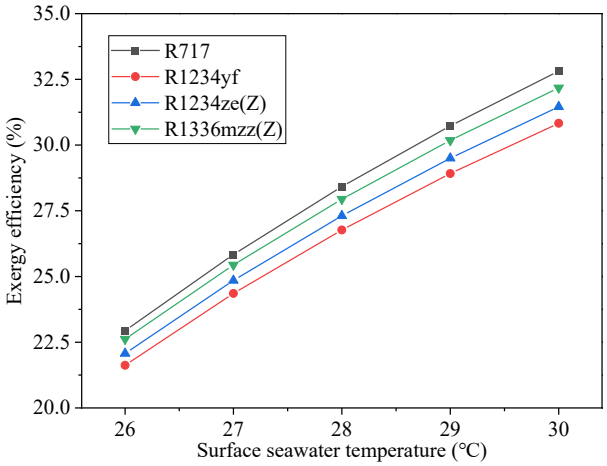

Figure 2. Exergy efficiency of OTEC system with various surface seawater temperatures.

Figure 3 shows the exergy efficiencies of OTEC systems using the four refrigerants as a function of cold seawater pumping depth, ranging from 400 to 1800 m. For all working fluids, the exergy efficiency gradually increases with increasing pumping depth. This trend is mainly due to the decreasing temperature of the cold seawater at greater depths, which expands the temperature difference driving the cycle and thus improves the system's exergy utilization. However, beyond approximately 1000 m, the rate of increase in exergy efficiency begins to slow down. This is because the temperature drop of deep seawater becomes less significant at greater depths, as deep ocean layers are less affected by solar heating. With increasing pumping depth, the temperature gradient rise diminishes, causing the exergy efficiency to increase at a slower rate. Among the four refrigerants, the ranking of exergy efficiency remains consistent across the pumping depth range: R717 exhibits the highest exergy efficiency, followed by R1336mzz(Z), R1234ze(Z), and R1234yf. From the exergy perspective, R717 remains the superior working fluid in terms of thermodynamic performance for OTEC systems under varying pumping depths.

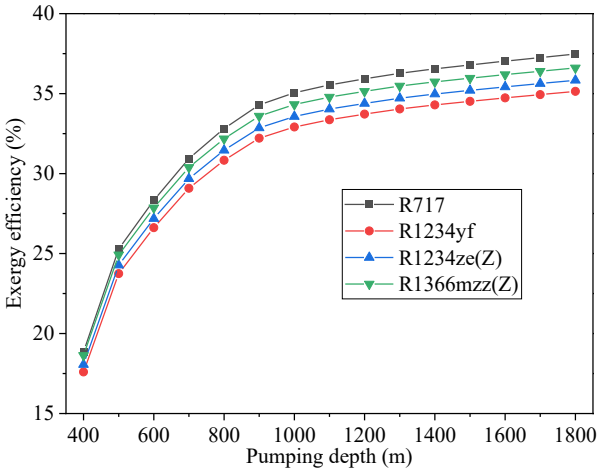

Figure 3. Exergy efficiency of OTEC system with various pumping depths.

Figure 4 shows the exergy destruction values of key components in OTEC systems using the four refrigerants, while Figure 5 presents the proportion of total exergy destruction attributed to each component. Among the refrigerants, R717 exhibits the lowest total exergy destruction at 111 kW, followed by R1336mzz(Z) at 115.3 kW, R1234ze(Z) at 115.9 kW, and R1234yf with the highest value of 116.8 kW. This trend is consistent with the observed exergy efficiencies. The advantage of R717 in minimizing exergy destruction mainly stems from its lower exergy destruction in the evaporator and the pump compared to the other refrigerants.

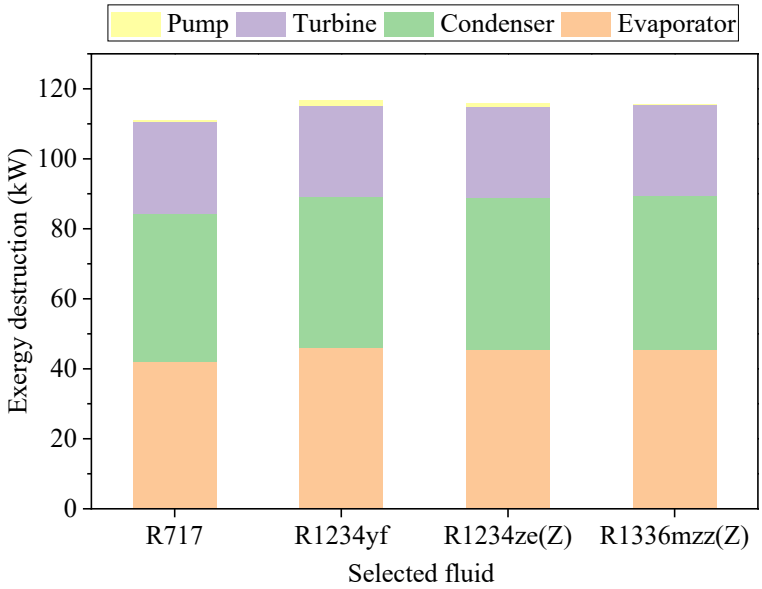

Figure 4. Exergy destruction in OTEC systems with various working fluids.

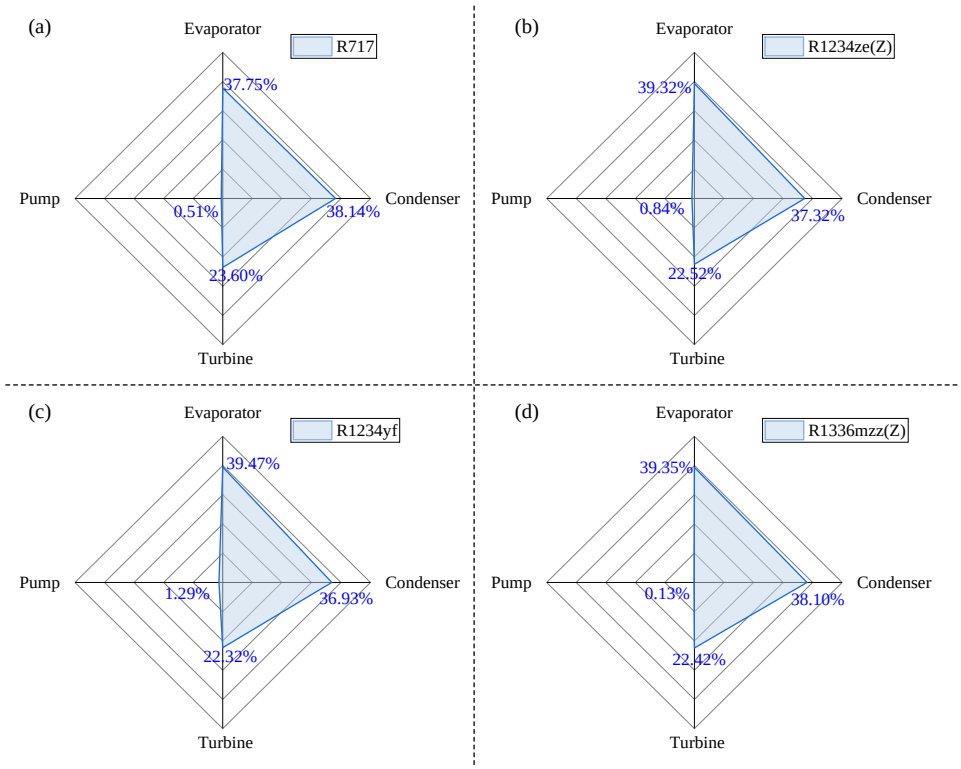

Figure 5. Proportion of exergy destruction across components in OTEC systems: (**a**) R717; (**b**) R1234ze(Z); (**c**) R1234yf; (**d**) R1336mzz(Z).

In summary, the exergy analysis reveals that R717 consistently delivers the highest thermodynamic performance and the lowest exergy destruction among the refrigerants considered, though the differences compared to low-GWP alternatives are relatively small. The distributions of exergy losses across system components are consistent with previous studies [15], and, as shown in Figure 5, the majority of exergy destruction occurs in the evaporator and condenser, followed by the turbine, while the pump contribution is negligible. These similarities highlight comparable thermodynamic behavior among the refrigerants. Given these findings, the assessment of low-GWP refrigerants as potential substitutes for R717 requires a broader evaluation beyond thermodynamics alone. Economic performance, environmental impact, and operational factors must also be carefully considered to determine their overall feasibility. Accordingly, the following section presents a detailed techno-economic analysis to complement the exergy study and support a more comprehensive refrigerant selection process.

4.2. Economic Analysis

4.2.1. Economic of Scale

The performance of an OTEC system is significantly influenced by its installed capacity. As capacity increases, economies of scale can be leveraged to reduce the *LCOE* and enhance financial returns. Figure 6 illustrates the relationship between installed capacity and two key economic indicators, *LCOE* and *NPV*. Figure 6a demonstrates that *LCOE* decreases with increasing installed capacity, reflecting the cost dilution effect, where fixed costs are spread over a larger power output. This trend is particularly pronounced in small-scale systems, where fixed costs constitute a substantial portion of total investment, leading to a more noticeable decline in *LCOE*. However, as capacity further increases, the rate of *LCOE* reduction slows down due to rising marginal costs of additional components and increased complexity in large-scale system implementation. Additionally, OTEC systems using ammonia exhibit lower *LCOE* across all capacity levels. This advantage primarily stems from ammonia's superior thermodynamic properties, which reduce the required heat exchanger area and pumping power. In contrast, OTEC systems using R1234yf and R1336mzz(Z) require larger heat exchanger areas to achieve similar performance levels, resulting in higher capital costs and *LCOE*. Notably, R1234ze(Z) has thermodynamic properties similar to ammonia, making the *LCOE* of OTEC systems using R1234ze(Z) closest to that of ammonia-based systems, even slightly lower in some cases.

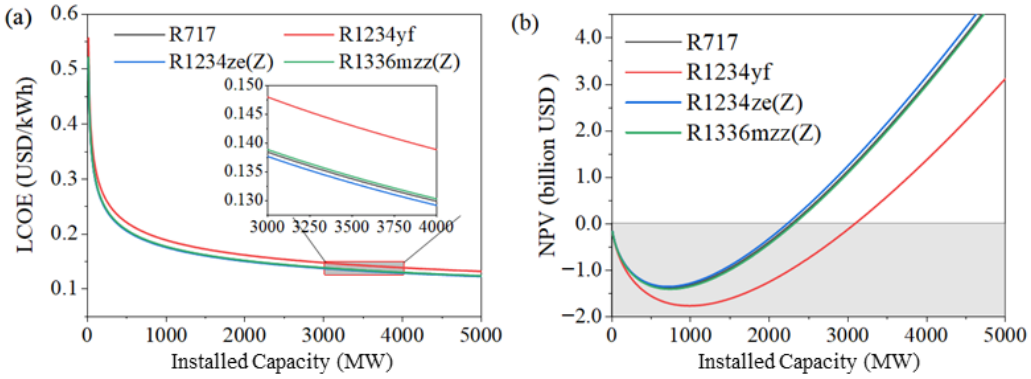

Figure 6. Economic of scale: (**a**) levelized cost of energy; (**b**) net present value (pumping depth = 800 m, surface temperature = 30 °C).

Figure 6b presents the variation in *NPV* across different installed capacities, indicating a trend where *NPV* initially decreases before increasing as capacity grows. This suggests that small-scale OTEC systems lack capital investment value, as additional investments yield diminishing returns. Only large-scale systems can generate greater financial benefits

from increased investment, making them more economically viable. The turning point at which the trend shifts varies depending on the working fluid. For ammonia, this transition occurs at 750 MW, while for OTEC systems using R1234yf, R1234ze(Z), and R1336mzz(Z), the turning points are 980 MW, 710 MW, and 730 MW, respectively.

The critical point where net present value equals zero ($NPV = 0$) is particularly significant, as it represents the minimum installed capacity required for an OTEC system to achieve financial breakeven over its operational lifetime. Figure 7 compares the critical installed capacities for OTEC systems using ammonia and environment-friendly working fluids under the conditions of an 800 m cold seawater pumping depth and a warm seawater temperature of 30 °C. The results indicate that the installed capacity required for $NPV = 0$ in an ammonia-based system is 2285 MW. Among the environment-friendly working fluids considered, R1234ze(Z) exhibits a lower critical installed capacity of 2225 MW, suggesting that OTEC systems using R1234ze(Z) can achieve financial breakeven at a smaller scale, thereby demonstrating both economic competitiveness and environmental advantage.

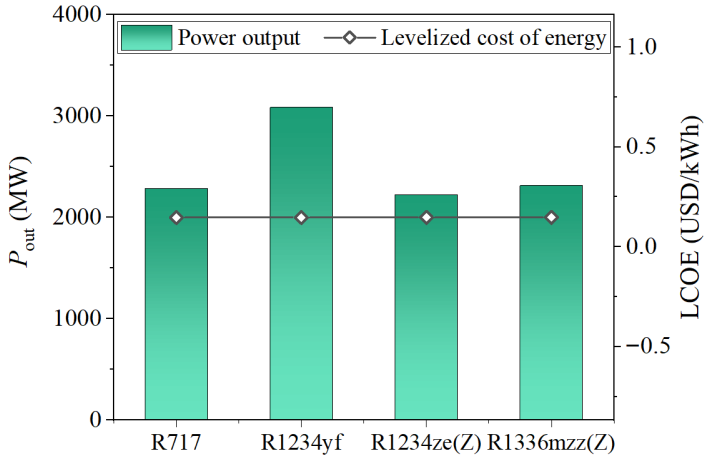

Figure 7. Comparison of installed capacity at zero net present value.

Furthermore, Figure 7 also shows that when *NPV* reaches zero, the system's *LCOE* is 0.147 USD/kWh, independent of the type of working fluid used. This finding highlights that while the choice of working fluid influences the required installed capacity to achieve financial feasibility, the breakeven *LCOE* remains constant across different working fluids.

To further compare the application potential of ammonia and R1234ze(Z) in OTEC systems across a wider range of conditions, Figure 8 examines the critical installed capacity under varying warm seawater temperatures and cold seawater pumping depths. The results show that as surface seawater temperature and cold seawater pumping depth increase, the critical installed capacity needed for financial breakeven gradually decreases. In terms of the differences between the two systems, at lower surface seawater temperatures and shallower cold seawater pumping depths, the critical installed capacities of ammonia- and R1234ze(Z)-based OTEC systems are quite similar. However, as the surface-seawater temperature increases and the pumping depth deepens, the difference between the two systems becomes more pronounced. Overall, the critical installed capacity is lower for the R1234ze(Z)-based system than for the ammonia-based system. For example, at a warm seawater temperature of 27 °C and a cold seawater pumping depth of 1000 m, both systems need an installed capacity of 4400 MW to reach financial breakeven. However, when the warm seawater temperature rises to 31 °C and the cold seawater pumping depth reaches 1800 m, the critical installed capacities decrease to 930 MW and 850 MW for ammonia and R1234ze(Z), respectively, with the latter being 8.6% lower.

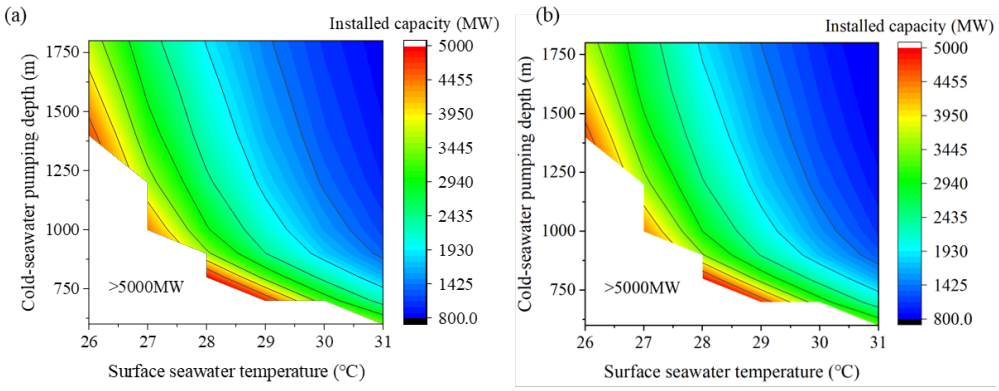

Figure 8. Installed capacity at zero net present value for OTEC system using (**a**) ammonia and (**b**) R1234ze(Z).

4.2.2. Effect of Cold Seawater Pumping Depth

Figure 9 illustrates the impact of cold seawater pumping depth on the *LCOE* across various installed capacities. The results indicate that, regardless of the working fluid type, the relationship between *LCOE* and pumping depth varies depending on the system scale. For large-scale systems (installed capacity $\geq$ 10 MW), *LCOE* decreases continuously with increasing pumping depth and eventually stabilizes at greater depths. Greater pumping depth yields colder seawater, increasing the effective temperature difference, which enhances cycle efficiency and lowers the *LCOE*. However, at sufficiently large depths, the additional gains in efficiency are gradually offset by the rising costs of pipeline construction and increased pumping power consumption, leading to a plateau in *LCOE* reduction.

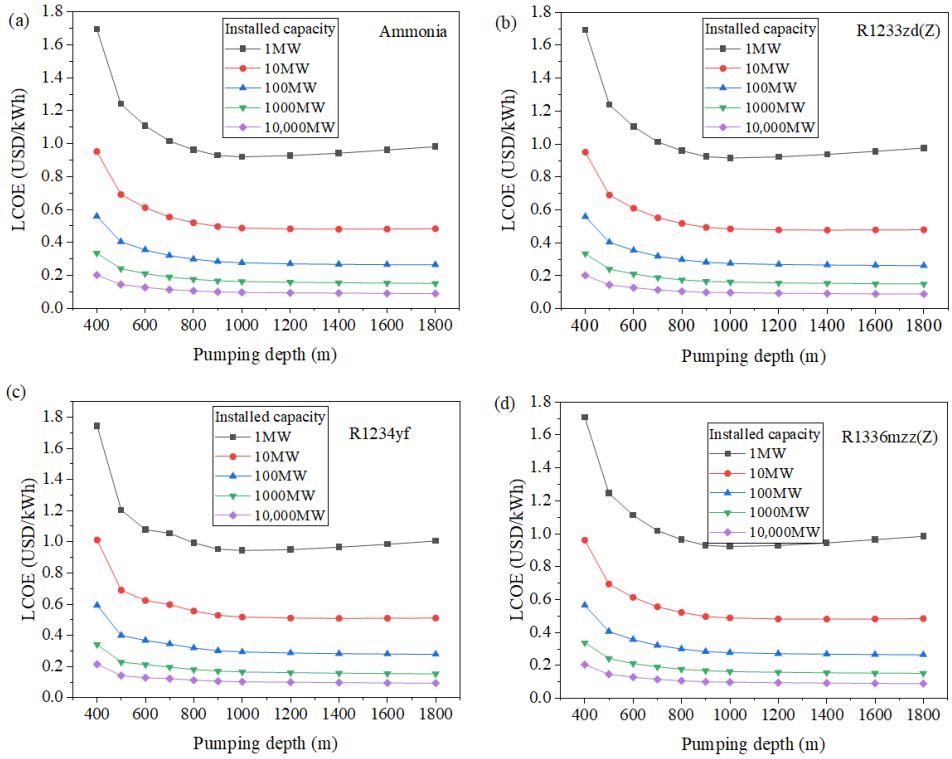

Figure 9. Levelized cost of energy of OTEC system with various pumping depth: (**a**) ammonia; (**b**) R1234ze(Z); (**c**) R1234yf; (**d**) R1233mzz(Z).

In contrast, for small-scale systems (installed capacity = 1 MW), *LCOE* initially decreases with increasing pumping depth before rising again. This occurs because the economic feasibility of small-scale OTEC systems is more sensitive to initial investment and

operational costs. While greater pumping depth initially lowers the *LCOE* by improving system efficiency, further depth increases result in a rise in pipeline investment and pumping energy consumption that outweighs the efficiency gains, causing *LCOE* to rise again. This suggests that, for small-scale OTEC systems, there exists an optimal pumping depth at which *LCOE* is minimized, typically in the range of 800–1000 m. Beyond this depth, the economic performance deteriorates. Therefore, in the design of small-scale OTEC systems, it is crucial to balance pumping depth and investment returns to determine the optimal cold seawater intake depth.

A comparison of the *LCOE* between the two systems reveals that, under the same pumping depth and installed capacity conditions, OTEC systems using ammonia generally exhibit higher *LCOE* than those using R1234zd(Z). This difference is particularly pronounced at smaller installed capacities (e.g., 1 MW and 10 MW). When the installed capacity reaches 1000 MW or higher, the *LCOE* gap between the two systems narrows, indicating that large-scale OTEC systems can effectively mitigate the economic differences associated with working fluid selection. Therefore, in practical engineering applications, a comprehensive optimization strategy considering working fluid properties, installed capacity, and pumping depth is essential to enhance the overall economic viability of OTEC systems.

4.2.3. Investment Breakdown

Having established the competitive advantages of R1234ze(Z) over ammonia, examining the capital distribution enables a more refined approach to optimizing OTEC system economics and reducing investment costs for various capacity ranges. As observed in Figure 10, the investment proportions of key components exhibit significant variations across different installed capacities, with distinct trends emerging as capacity increases. These trends provide valuable insights for optimizing OTEC system design by identifying cost-intensive components for cost reduction.

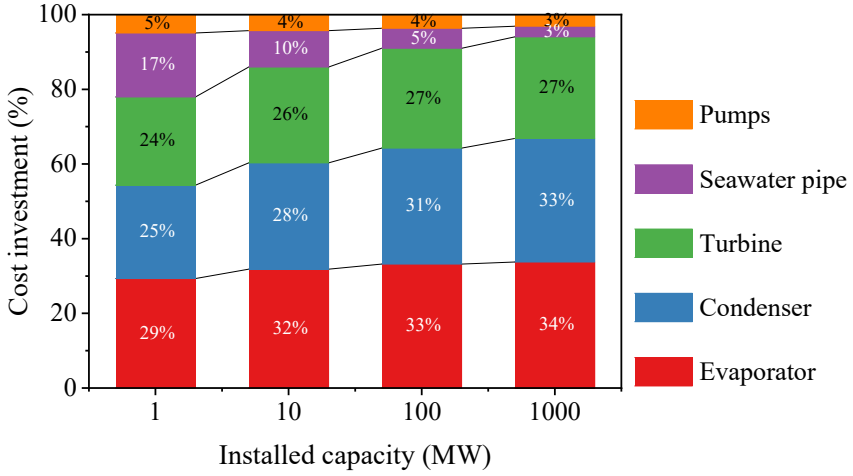

Figure 10. Investment breakdown of OTEC system using R1234ze(Z).

Firstly, the investment proportion of evaporators and condensers increases with the installed capacity. The evaporator's share of total investment rises from 29% at 1 MW to 34% at 1000 MW, while the condenser's share increases from 25% to 33%. This trend suggests that in large-scale OTEC systems, heat exchanger costs account for a growing portion of total investment. Therefore, optimizing the structure and materials of heat exchangers is crucial for cost reduction in large-scale OTEC design. Secondly, the investment proportion of turbines remains relatively stable across different installed capacities, ranging from 24% to 27%. This indicates that, despite the increase in OTEC system scale, turbines

remain a major component of system investment, with their cost share not significantly decreasing as capacity expands. This stability may be attributed to the fact that turbine design is constrained by working fluid properties, operating parameters, and material costs, leading to a consistent investment proportion across different scales of OTEC systems. The investment share of seawater pipelines decreases significantly as installed capacity increases, dropping from 17% at 1 MW to 3% at 1000 MW. This suggests that in large-scale OTEC systems, the unit cost of seawater transportation infrastructure decreases, primarily due to economies of scale. In lower systems, optimized pipeline layout, improved transport efficiency, and lower installation costs contribute to reduced relative investment in seawater pipelines. Enhancing pipeline design and selecting cost-effective materials can further help lower investment costs in OTEC systems. Regardless of the system scale, the investment proportion of pumps remains relatively small and has a minimal impact on total capital expenditure. Therefore, excessive consideration of pump costs in the overall investment optimization process is unnecessary.

In summary, as the installed capacity of OTEC systems increases, the investment proportion of evaporators and condensers increases, while the share allocated to seawater pipelines and pumps decreases, and the turbine investment remains relatively stable. This indicates that for small-scale OTEC systems, optimization efforts should focus on improving the design and efficiency of seawater pipelines to reduce costs. In contrast, for large-scale OTEC systems, reducing the cost of heat exchangers is the key measure to enhance economic feasibility.

5. Conclusions

This study first evaluates the thermodynamic performance of environment-friendly working fluids and conventional ammonia in OTEC systems through exergy analysis. Building on this foundation, a detailed techno-economic assessment is then carried out, with particular emphasis on R1234ze(Z), whose economic performance is found to be comparable to that of R717. The analysis includes considerations of economies of scale, the impact of pumping depth, and capital investment distribution. Based on the comprehensive evaluation, three key conclusions can be drawn:

(1) R1234ze(Z) offers significant environmental advantages, featuring a low global warming potential and non-toxic properties. Although its exergy efficiency is slightly lower than that of ammonia, OTEC systems using R1234ze(Z) achieve a lower levelized cost of energy (*LCOE*). Furthermore, the critical installed capacity required for financial breakeven in R1234ze(Z)-based systems is 8.6% lower than that of ammonia-based systems.

(2) The impact of pumping depth on economic performance is significant and differs between small- and large-scale systems. For small-scale systems (installed capacity = 1 MW), *LCOE* initially decreases with increasing pumping depth but subsequently rises. In contrast, for large-scale systems (installed capacity $\geq$ 10 MW), *LCOE* decreases with increasing pumping depth and eventually stabilizes.

(3) Capital investment distribution in OTEC systems varies with installed capacity. In small-scale systems, seawater pipelines represent a substantial share of investment but decrease rapidly with increasing capacity. Therefore, optimization efforts in small-scale OTEC plants should focus on the layout and efficiency of seawater pipelines, while in large-scale systems, reducing the cost of heat exchangers is the key measure to enhance economic feasibility.

Author Contributions: H.L.: Investigation, writing—original draft; C.F.: methodology, writing—original draft; D.L.: writing—original draft; Y.C.: conceptualization; F.Y.: writing—original draft, software, funding acquisition. All authors have read and agreed to the published version of the manuscript.

Funding: The authors would like to express their appreciation for the funding support of the National Natural Science Foundation of China (Nos. 51906170).

Data Availability Statement: Data will be made available on request.

Conflicts of Interest: The authors declare no conflicts of interest.

Abbreviations

The following abbreviations are used in this manuscript:

LCOE	Levelized cost of energy
OTEC	Ocean thermal energy conversion
NPV	Net present value
HDPE	High-density polyethylene
CRF	Capital recovery factor

References

1. Du, T.; Jing, Z.; Wu, L.; Wang, H.; Chen, Z.; Ma, X.; Gan, B.; Yang, H. Growth of ocean thermal energy conversion resources under greenhouse warming regulated by oceanic eddies. *Nat. Commun.* **2022**, *13*, 7249. [CrossRef] [PubMed]
2. Gao, W.; Wang, F.; Zhang, Y.; Tian, Z.; Wu, D.; Farrukh, S. Review of performance improvement strategies and technical challenges for ocean thermal energy conversion. *Appl. Therm. Eng.* **2025**, *266*, 125506. [CrossRef]
3. Liu, W.; Xu, X.; Chen, F.; Liu, Y.; Li, S.; Liu, L.; Chen, Y. A review of research on the closed thermodynamic cycles of ocean thermal energy conversion. *Renew. Sustain. Energy Rev.* **2020**, *119*, 109581. [CrossRef]
4. Lee, H.-S.; Lee, S.-W.; Kim, H.-J.; Jung, Y.-K. Performance characteristics of 20 kW ocean thermal energy conversion pilot plant. In Proceedings of the ASME 2015 9th International Conference on Energy Sustainability collocated with the ASME 2015 Power Conference, the ASME 2015 13th International Conference on Fuel Cell Science, Engineering and Technology, and the ASME 2015 Nuclear Forum, San Diego, CA, USA, 28 June–2 July 2015; American Society of Mechanical Engineers: New York, NY, USA, 2025; Volume 56840, p. V001T07A2.
5. Kusuda, E.; Morisaki, T.; Ikegami, Y. Performance Test of Double-stage Rankine Cycle experimental plant for OTEC. *Procedia Eng.* **2015**, *105*, 713–718. [CrossRef]
6. Lu, B.; Yu, Y.; Tian, M.; Chen, Y.; Zhang, L.; Liu, Y. Experimental study of a high-power generation platform for ocean thermal energy conversion. *Energy* **2024**, *309*, 133115. [CrossRef]
7. Lu, B.; Liu, Y.; Zhai, X.; Zhang, L.; Chen, Y. Design and Experimental Study of 50 kW Ocean Thermal Energy Conversion Test Platform Based on Organic Rankine Cycle. *J. Mar. Sci. Eng.* **2024**, *12*, 463. [CrossRef]
8. Martin, B.; Okamura, S.; Yasunaga, T.; Ikegami, Y.; Ota, N. OTEC and advanced deep ocean water use for Kumejima: An introduction. In Proceedings of the OTEC and Advanced Deep Ocean Water Use for Kumejima: An Introduction, Chennai, India, 21–24 February 2022; IEEE: New York, NY, USA, 2022; pp. 1–5.
9. Koto, J. Potential of ocean thermal energy conversion in Indonesia. *Int. J. Environ. Res. Clean Energy* **2016**, *4*, 1–7.
10. Hu, Z.; Chen, Y.; Zhang, C. Role of R717 blends in ocean thermal energy conversion organic Rankine cycle. *Renew. Energy* **2024**, *221*, 119756. [CrossRef]
11. Yang, M.-H.; Yeh, R.-H. Investigation of the potential of R717 blends as working fluids in the organic Rankine cycle (ORC) for ocean thermal energy conversion (OTEC). *Energy* **2022**, *245*, 123317. [CrossRef]
12. Zhang, Y.; Liu, J.; Liu, Z. Thermo-economic examination of ocean heat-assisted pumped thermal energy storage system using transcritical CO_2 cycles. *Appl. Therm. Eng.* **2024**, *255*, 123992. [CrossRef]
13. Yilmaz, F. Energy, exergy and economic analyses of a novel hybrid ocean thermal energy conversion system for clean power production. *Energy Convers. Manag.* **2019**, *196*, 557–566. [CrossRef]
14. Assareh, E.; Assareh, M.; Alirahmi, S.M.; Jalilinasrabady, S.; Dejdar, A.; Izadi, M. An extensive thermo-economic evaluation and optimization of an integrated system empowered by solar-wind-ocean energy converter for electricity generation—Case study: Bandar Abas, Iran. *Therm. Sci. Eng. Prog.* **2021**, *25*, 100965. [CrossRef]
15. Sun, F.; Ikegami, Y.; Jia, B.; Arima, H. Optimization design and exergy analysis of organic rankine cycle in ocean thermal energy conversion. *Appl. Ocean Res.* **2012**, *35*, 38–46. [CrossRef]

16. Yoon, J.-I.; Son, C.-H.; Baek, S.-M.; Kim, H.-J.; Lee, H.-S. Efficiency comparison of subcritical OTEC power cycle using various working fluids. *Heat Mass Transf.* **2014**, *50*, 985–996. [CrossRef]
17. Vera, D.; Baccioli, A.; Jurado, F.; Desideri, U. Modeling and optimization of an ocean thermal energy conversion system for remote islands electrification. *Renew. Energy* **2020**, *162*, 1399–1414. [CrossRef]
18. Huo, E.; Chen, W.; Deng, Z.; Gao, W.; Chen, Y. Thermodynamic analysis and optimization of a combined cooling and power system using ocean thermal energy and solar energy. *Energy* **2023**, *278*, 127956. [CrossRef]
19. Fan, C.; Chen, Y. Design Optimization of Ocean Thermal Energy Conversion (OTEC) Considering the Off-Design Condition. *J. Therm. Sci.* **2023**, *32*, 2126–2143. [CrossRef]
20. Kakaç, S.; Liu, H.; Pramuanjaroenkij, A. *Heat Exchangers: Selection, Rating, and Thermal Design*; CRC Press: Boca Raton, FL, USA, 2002.
21. Nilpueng, K.; Wongwises, S. Experimental study of single-phase heat transfer and pressure drop inside a plate heat exchanger with a rough surface. *Exp. Therm. Fluid Sci.* **2015**, *68*, 268–275. [CrossRef]
22. Fan, C.; Zhang, C.; Gao, W. Improving the ocean thermal energy conversion by solar pond. *Sol. Energy* **2024**, *274*, 112583. [CrossRef]
23. Langer, J.; Ferreira, C.I.; Quist, J. Is bigger always better? Designing economically feasible ocean thermal energy conversion systems using spatiotemporal resource data. *Appl. Energy* **2022**, *309*, 118414. [CrossRef]
24. Vega, L.A.; Michaelis, D. First generation 50 MW OTEC plantship for the production of electricity and desalinated water. In Proceedings of the Offshore Technology Conference, Houston, TX, USA, 3–6 May 2010; OTC: Springfield, MO, USA, 2010; p. OTC-20957-MS.